Received: 8 June 2022 | Accepted: 25 October 2022

DOI: 10.1002/vzj2.20239

Vadose Zone Journal

ORIGINAL RESEARCH ARTICLE

Nitrate contamination of urban groundwater and heavy rainfall: Observations from Dakar, Senegal

Abdoulaye Pouye[1] | **Seynabou Cissé Faye**[1] | **Mathias Diédhiou**[1] | **Cheikh Becaye Gaye**[1] | **Richard G. Taylor**[2]

[1]Geology Dep., Faculty of Sciences and Techniques, Univ. Cheikh Anta Diop, B.P. 5005, Dakar-Fann, Senegal

[2]Dep. of Geography, Univ. College London, Gower Street, London WC1E 6BT, United Kingdom

Correspondence
Abdoulaye Pouye, Geology Dep., Faculty of Sciences and Techniques, Univ. Cheikh Anta Diop, Dakar, B.P. 5005, Dakar-Fann, Senegal.
Email: abdoulaye8.pouye@ucad.edu.sn

Assigned to Associate Editor Kenton Rod.

Funding information
ANSTS (Académie Nationale des Sciences et Techniques du Sénégal); Royal Society - DFID Africa Capacity Building, Grant/Award Number: AQ140023

Abstract

In low-income urban areas of major cities in Africa, sanitation provision derives primarily from onsite systems often comprising septic tanks and pit latrines. Such systems rely upon the ability of the surrounding soil and substratum to attenuate contaminants like nitrate and pathogenic microorganisms in wastewater. Here, we assess soil–water and solute dynamics in Quaternary aeolian sands underlying a densely populated suburb (Keur Massar) of Dakar (Senegal) using high-frequency monitoring and vadose zone modeling (Hydrus-1D). Observations of rainfall intensity, soil moisture content, and shallow groundwater-level fluctuations and nitrate concentrations were carried out at an experimental site adjacent to a septic tank supplied by toilets used by a primary school. Rapid rises in soil moisture content and episodic recharge contributions observed in groundwater levels caused by heavy (>10 mm h^{-1}) and extreme (>20 mm h^{-1}) rainfall are well modeled (R^2 = .79–.83; RMSE = 0.012–0.019) by pore-matrix flow in the unsaturated zone by the Darcy–Richards equation. Spot sampling around the most intense rainfall of 2020 (45 mm h^{-1}) reveals a fivefold rise and fall in the concentration of nitrate in soil moisture (~500 to ~2,500 mg L^{-1}). These measurements provide new insight into the hydrological dynamics by which shallow groundwater is grossly contaminated (>500 mg L^{-1}) by nitrate through episodic flushing by heavy rainfall of wastewater from a vast estimated network of over 250,000 septic tanks underlying this suburb of Dakar.

1 | INTRODUCTION

Shallow groundwater plays a vital role in the provision of water supplies in low-income areas of urban Africa (Gaye & Tindimugaya, 2019; Lapworth et al., 2017; Xu et al., 2019). Use of urban groundwater to improve access to safe water is threatened by not only overpumping, depleting groundwater storage, but also contamination from human activity (Diouf et al., 2012). One of the primary risks to urban groundwater quality is that posed by low-cost onsite sanitation systems such as pit latrines and septic tanks that exploit the shallow subsurface for the disposal and containment of human excreta (Diaw et al., 2020; Kulabako et al., 2007; Nayebare et al., 2020; Okotto-Okotto et al. 2015; Sorensen, Carr, et al., 2020; Taylor et al., 2009; Twinomucunguzi et al., 2020). Sustaining

Abbreviations: VG, van Genuchten–Mualem; VMC, volumetric water content.

conjunctive use of the subsurface for onsite water supply and sanitation provision is especially challenging under conditions of rapid urbanization (Lapworth et al., 2017). Currently, 41% of the population of sub-Saharan Africa lives in urban areas (World Bank, 2020), with a mean urban growth rate of 4% in 2020.

In dryland areas of sub-Saharan Africa, groundwater recharge occurs disproportionately from heavy, often extreme rainfall (Cuthbert et al., 2019; Goni et al., 2021; Seddon et al., 2021; Taylor et al., 2013). The mechanisms by which water surpluses from heavy rainfall events are transmitted to groundwater are often unclear but have been shown to include: (a) focused recharge via leakage from ephemeral streams or ponds (Favreau et al., 2009; Goni et al., 2021; Seddon et al., 2021), (b) rapid infiltration via macropores in low-permeability weathered soils (Beven & Germann, 2013; Owor et al., 2009; Sorensen et al., 2021), and (c) permeable Quaternary sands (Cissé Faye et al., 2019; Goni et al., 2021; Kotchoni et al., 2019). Rapid responses in groundwater levels to heavy rainfalls observed from collated piezometric records in many of these cited studies have highlighted the vulnerability of groundwater to contamination.

In the shallow unconfined aquifer of Quaternary sands underlying Dakar (Senegal), previous research has revealed widespread and substantial contamination of shallow groundwater by nitrate in the low-income suburb of Dakar (Thiaroye) where observed concentrations can exceed 500 mg L^{-1} (Cissé Faye et al., 2004; Diaw et al., 2020; Madioune et al., 2011; Tandia, 2000). The origin of nitrate in groundwater has been traced to fecal sources using stable-isotope ratios of N and O (Diedhiou et al., 2012; Re et al., 2010). Sanitation provision in this low-income suburb is onsite and comprises almost entirely septic tanks. Here, Diaw et al. (2020) mapped an estimated 253,000 septic tanks over an area of 520 km^2 with densities ranging from 1 to 70 per hectare. Mapping further revealed a statistically significant relationship between the density of onsite sanitation facilities and observed nitrate concentrations in shallow groundwater. The processes and hydrodynamics by which effluent from onsite sanitation is transported to groundwater remain inadequately understood.

Recent establishment of a dedicated observatory in suburban Dakar to monitor hydrological and hydrochemical changes from the land surface through the unsaturated zone to groundwater at a school served by a large septic tank facility has yielded new, high-frequency observations of the dynamics of subsurface transmission of nitrate from its source (i.e., septic tank effluent) to receptor (i.e., well). Here, we interrogate observations conducted from April to November 2020, paying particular attention to the hydrological dynamics associated with heavy (>10 mm h^{-1}) and extreme (>20 mm h^{-1}) rainfall events during the rainy season. The main aim is to understand how aqueous fecal contaminants like nitrate are mobilized from onsite sanitation facilities and contaminate underlying groundwater in a densely populated urban environment and thereby inform improved urban groundwater and sanitation management strategies. The study also seeks to resolve the nature of flow in the unsaturated zone and specifically whether nitrate transmission occurs via pore-matrix flow, consistent with the assumptions of Darcy–Richards equation, or preferential pathways (e.g., soil macropores) bypassing the soil matrix.

Core Ideas

- Soil-water and solute dynamics were assessed by high-frequency monitoring and vadose-zone modelling.
- High-frequency monitoring was conducted at an experimental site adjacent to a septic tank.
- Heavy rainfall events (>10 mm hr^{-1}) cause the leaching of wastewater from the septic tank to groundwater.
- Observations show the contribution of septic systems and rainfall to groundwater contamination by nitrate.

2 | MATERIAL AND METHODS

2.1 | Local setting

The study area is located in the Keur Massar district, a suburb of Dakar in Senegal (Figure 1). This densely populated area with an estimated population of 203,000 inhabitants spread over 25 km^2 (ANSD, 2013) is a low-income community served by onsite sanitation, comprising overwhelmingly septic tanks. The climate is semiarid and annual rainfall (mean = 410 mm, 1961–1990) varies substantially (e.g., 150 mm in 1983, 723 mm in 2009). Maximum air temperatures (mean = 29.5 °C, 1980–2010) occur between May and June as well as October and November around the beginning and end of the rainy season (Diouf et al., 2020). The study area is located above an unconfined aquifer of Quaternary sand that extends along the northern coastal zone of Senegal from Dakar. The Quaternary sand aquifer comprises sands and sandy-clay lenses of aeolian origin, which form the Ogolian dunes in the coastal zone. Groundwater recharge tends to occur during extreme precipitation events and is diffuse, as indicated by previous research (Antea-Senagrosol, 2003; Cissé Faye et al., 2001, 2019).

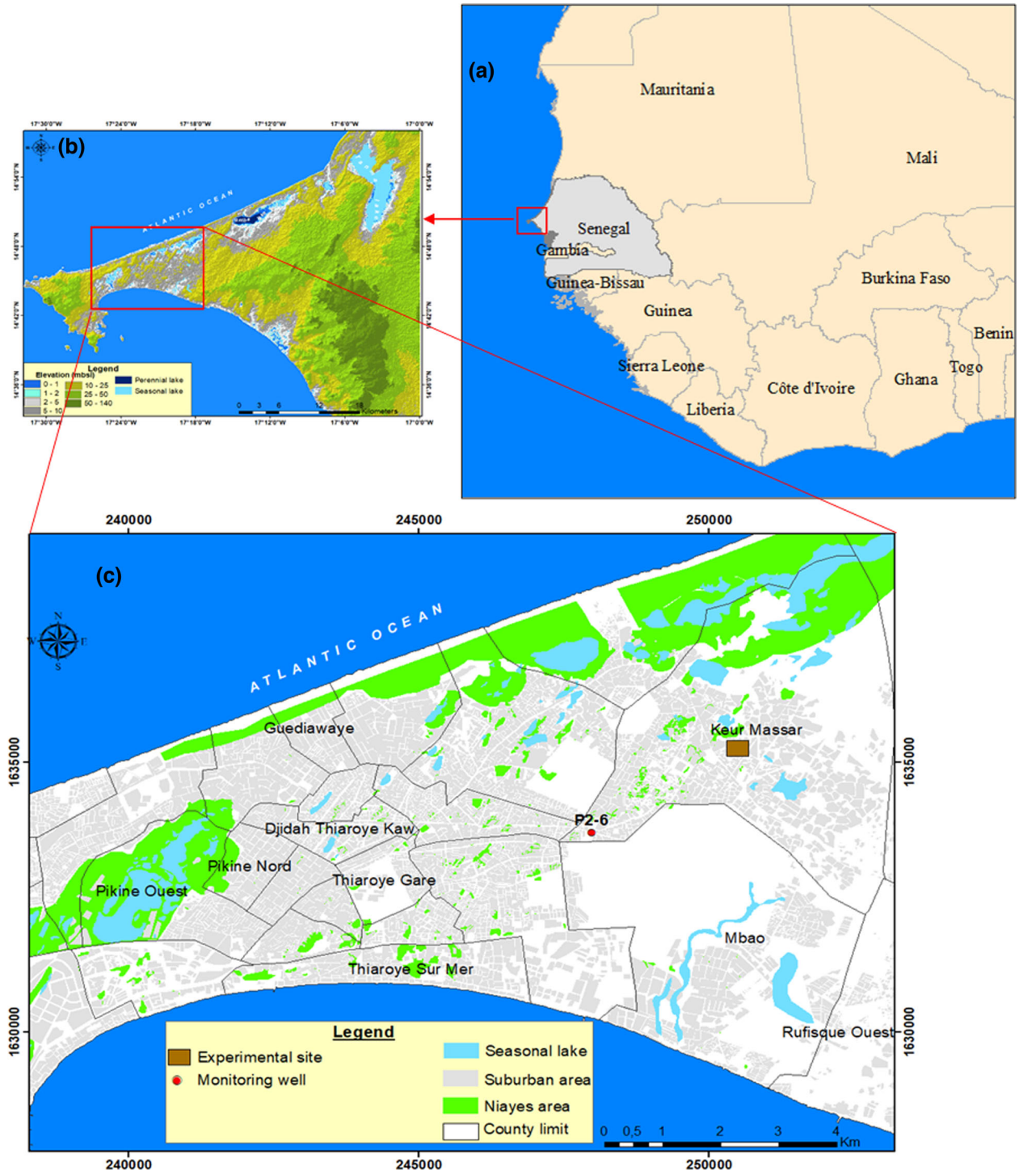

FIGURE 1 Series of maps showing the locations respectively of (a) Senegal, (b) Cap Vert Peninsula, and (c) Keur Massar in suburban Dakar

2.1.1 | Field experiments and monitoring

Field experiments were conducted near a septic tank used to collect fecal raw and wastewater in a primary school (Ecole élémentaire parcelles assainies unité 3) with 530 pupils in the suburb of Keur Massar (Figure 1). The onsite sanitation system comprises a sanitary block with six toilets and a septic tank that is 6.5 m (length) × 2 m (width) and installed 2 m into the ground (Figure 2). The tank receives wastewater from the toilet block via collectors connected by polyvinyl chloride (PVC) pipes and downstream via twin sumps for wastewater evacuation through the soil (Figure 2). Raw wastewater from cabins first converges towards the first collector where it then continues to the second collector before reaching the septic

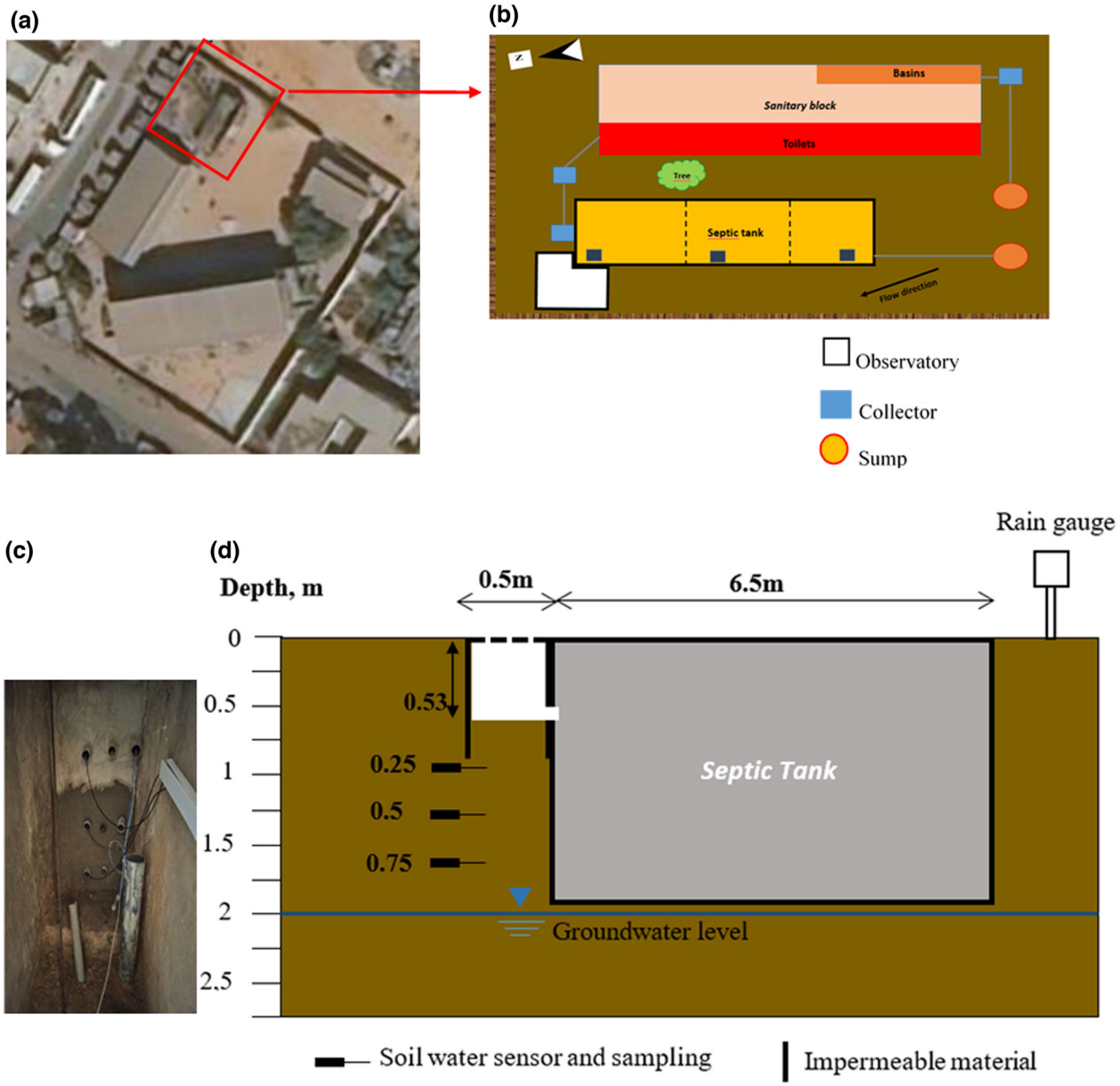

FIGURE 2 (a) Experimental field in Keur Massar within the Dakar suburb ESRI image; (b) schematic presentation of onsite sanitation system and the experimental device; (c) photo of vertical layout of soil moisture monitoring and sampling, and (d) schematic diagram showing the vertical arrangement of monitoring devices and pore water sampling (0.0-to-2.75-m depth)

tank. The second collector, which measures 0.5 × 0.5 m square and is 0.53 m deep, leaks so that raw wastewater can infiltrate before it reaches the septic tank. Site investigations focused on leakage from this collector, as pollutants are released directly into the soil before anaerobic treatment is initiated into the septic tank. To monitor water dynamic from the onsite sanitation system to the groundwater, soil moisture (capacitance) probes and tensiometers were installed at 0.25, 0.50, and 0.75 m below the top of the collector (0.53 m below ground) so that total installed depths of soil-moisture probes are 0.78, 1.03, and 1.28 m below ground. At these same levels, suction cups were also installed to collect pore-water samples. A rain gauge was implemented inside the site to quantify precipitation (Figure 2). Monitoring of groundwater-level fluctuations in the unconfined aquifer was carried out in a piezometer near (2 km) the experimental site. During the whole monitoring process, hourly data were collected at all devices.

2.1.2 | Measurement and analysis

Soil sampling was carried out inside the experimental site. Samples of 100 ml (cm^3) were taken close to the septic tank with an Eijelkamp soil sample ring kit auger each 50 cm

TABLE 1 Particle size, bulk density (BD), total porosity (TP), and texture from unsaturated zone of quaternary sand aquifer

	Soil particle size					
Soil depth	Sand	Silt	Clay	BD	TP	Texture
cm	———	%	———	g cm^{-1}	%	
0	94	4	2	1.65	41	Sandy
50	95	2	3	1.65	41	Sandy
100	97	1	2	1.65	43	Sandy
150	98	1	1	1.64	41	Sandy
200	96	0	4	1.60	43	Sandy

from the soil surface to the capillary fringe (2 m). Samples were then oven dried at the Universite Cheikh Anta Diop hydrochemistry laboratory to determine the total porosity and bulk density (by gravimetric method), as well as soil texture by the hydrometer experimentation (Table 1). Soil physical parameters are used to assess soil hydraulic properties.

Hourly meteorological data including rainfall amount and air temperature were collected by the Lambrecht tipping-bucket rain gauge (Lambrecht meteo). Groundwater-level data were recorded in an observation piezometer at 2 km to the experimental site (Figure 2) by an AquaTroll 200 data logger (In-Situ) from April 2020 to February 2021. Monitoring soil volumetric water content (VMC) was carried out from 22 Apr. to 30 Nov. 2020. This period covers two dry seasons on either side of the 2020 monsoon. Soil water capacitance probes (Water Scout 300, Spectrum Technologies) were deployed at depths of 0.78, 1.03, and 1.28 m below ground (25-cm intervals); data were recorded by WatchDog 1000 Series Micro Stations logger (Spectrum Technologies). In addition, hourly pressure head measurements were performed by the T8 tensiometer (UMS GmbH) at the same depth intervals. Pressure head data were recorded via CR300 data logger (Campbell Scientific). Soil water retention curves were assessed using in situ measurements of VMC and pressure head.

Soil water sampling was carried at the same depths of soil moisture monitoring. Pore waters were extracted via plastic suction cup (Eijelkamp) and collected during the monsoon in August and September 2020. Before sampling, a 75-kPa pressure was induced by an Eijelkamp vacuum pump the day before sampling. After each sampling, the residual solution was evacuated by injection. In order to assess short-time chemical variability, two samples were taken on 28 Aug. 2020. Sampling was carried out just 2 h after application of the pressure extraction (9:00 a.m. and 2:30 p.m.). All water samples were filtered through a 0.2-µm membrane filter before analyses by HACH DR 6000 spectrophotometer to assess aqueous concentrations of N compounds (nitrates, nitrites, and ammonium), total organic C, phosphates, and total Fe concentrations (Table 2).

2.2 | Hydrological modeling

Hydrological modeling was used to test conceptual understanding of water flow in the study area using the Richards equation for variably saturated porous media.

2.2.1 | Hydrus-1D model description

The one-dimensional numerical model Hydrus-1D (Šimůnek et al., 2008) was used to simulate soil water dynamics through the unsaturated porous media. The governing equation for one dimension water flow is described by the Richards equation as below:

$$\begin{cases} \frac{\partial \theta}{\partial t} = \frac{\partial q}{\partial z} \\ \frac{\partial q}{\partial z} = -\frac{\partial}{\partial z}\left[K_s\left(\frac{\partial h}{\partial z}+1\right)\right] - S \end{cases} \quad (1)$$

where θ is the volumetric water content (VMC in cm^3 cm^{-3}), q the water flux density (cm h^{-1}), h the pressure head in the porous media (cm), t is the time (h), K_s is the saturated hydraulic conductivity (cm h^{-1}), z is the spatial coordinate negative downward (cm), and S the sink term representing the plant water uptake. Solving Equation 1 depends on the nonlinear relationship between VMC, pressure head, and hydraulic conductivity described by the van Genuchten–Mualem (VG) equation shown Equations 2 and 3 below:

$$\theta_h = \begin{cases} \theta_r + \frac{\theta_s - \theta_r}{(1+|\alpha h|^n)^m}, & h < 0 \\ \theta_s, & h \geq 0 \end{cases} \quad (2)$$

where $m = 1 - 1/n$ and $n > 1$, and

$$K_h = K_s\, S_e^l\left[1 - \left(1 - S_e^{\frac{1}{m}}\right)^m\right]^2 \quad (3)$$

where $S_e = (\theta - \theta_r)/(\theta_s - \theta_r)$, θ_r and θ_s (cm^3 cm^{-3}) are the residual and saturated VMC respectively, α (cm^{-1}) is an air entry parameter, n (–) is a pore size distribution, l is the pore connectivity, and S_e is the effective saturation (cm^3 cm^{-3}).

2.2.2 | Hydrus-1D implementation

The conceptual model representing the vadose zone in the study area's Quaternary medium sand is a single homogeneous layer of 1.5 m in thickness. Simulations were processed during rainy season 2020 (from 12 June to 12 Oct. 2020) with hourly time step. In order to estimate the VG parameters, soil water retention curves were assessed by (a) indirect estimation, based on existing surrogate data translation (i.e., texture and bulk density) into soil hydraulic parameters (Schaap et al.,

TABLE 2 Depth-time-dependent variability of organic matter (TOC), N compounds (NO_3^-, NO_2^-, and NH_4^+), phosphates (PO_4^{3-}), and total Fe

Soil depth	TOC	NO_3^-	NO_2^-	NH_4^+	PO_4^{3-}	Total Fe
m	mg L^{-1}					
0.78	179–350	341–952	9–36	0.7–1	48–53	0.9–1.3
1.03	183–350	84–2,376	5–27	0.1–1	16–28	0.4–2.3
1.28	185–319	391–2,692	1–11	0.4–1	13–24	1.2–1.7

2001), and (b) field measurements of VMC and pressure head, modeled via the retention curves model. The hydraulic parameters inferred via field assessment of soil water retention curves were then optimized using inverse solutions focused on high frequency soil moisture content as input parameter. This procedure implements a Marquardt–Levenberg type parameter estimation technique for inverse estimation of hydraulic properties (Šimůnek & Hopmans, 2002; Šimůnek et al., 2016). The calibrated hydraulic parameters were then used to simulate VMC through the unsaturated zone during monsoon. Variably atmospheric boundary conditions were imposed as upper boundary conditions, whereas we assumed free drainage boundary conditions from the bottom as groundwater does not influence the domain. Evapotranspiration was neglected in the modeling because of the imperviousness of the soil surface. The observed VMC recorded on 12 June was used as the initial boundary condition. The model performance was assessed via RMSE and R^2 as outlined in Equations 4 and 5 below:

$$\mathrm{RMSE} = \sqrt{\frac{1}{n}\sum_{i=1}^{n}\left(S_i - O_i\right)^2} \tag{4}$$

$$R^2 = \left[\sum_i^n (O_i - \bar{O})(S_i - \bar{S})\right]^2 / \left[\sum_{i=1}^n \left(O_i - \bar{O}\right)^2 \sum_{i=1}^n \left(S_i - \bar{S}\right)^2\right] \tag{5}$$

where n is the number of paired observations, O_i and S_i are the observed and simulated values, respectively, and $\bar{O}$ and $\bar{S}$ are the mean of the observed and simulated values, respectively.

3 | RESULTS

3.1 | Observed hydrological changes through the unsaturated zone

Monitoring of rainfall, VMC, and groundwater levels was conducted from 22 April to 30 November 2020 (Figure 3). Time series observations are divided into three parts: (a) a test phase during which baseline (reference) conditions are resolved during the dry season (22 Apr. to 12 June 2020) before the operation of newly constructed toilets during the COVID pandemic (6 Mar. 2020); (b) rainy season monitoring during which rain events of varying intensity influence soil moisture and groundwater levels (13 June to 14 Oct. 2020); and (c) dry season monitoring during which toilets generated effluent but no rainfall occurred (15 Oct. to 30 Nov. 2020).

Figure 4 shows hourly variations with depth of in situ soil moisture as VMC with depth within the unsaturated zone after the installation of probes from 22 Apr. to 12 June 2020. These measurements, together with groundwater levels (meters below ground level), occur during the dry season when no rain fell and toilets draining to the septic tank were not operational (i.e., not producing or discharging effluent). Changes in soil moisture consequently derived from deliberate experiments conducted prior to the opening of the school on 2 June 2020. Time series data resolve well baseline (i.e., residual) soil moisture with depth in the absence of moisture inputs; mean VMC values are 0.05, 0.04, and 0.03 at depths of 0.78, 1.03, and 1.28 m, respectively. Episodic peaks during the testing phase result from spaced inflows via toilets draining to the septic tank over short periods (pulses) of 2–6 h. Resultant peaks were recorded between 9:00 a.m. and 12:00 p.m. in which soil moisture rose by values ranging from 0.08 (12 June) to 0.21 (27 May). During these wetting processes, the soil was never fully saturated (<0.42). Depth variations in soil moisture trace the passing of the moisture front through the unsaturated zone. Observations at 1.03 and 1.28 m reveal pulses that follow each other in time but with much smaller amplitudes except for the experiment on 27 May 2020 when, curiously, increases in soil moisture at 1.03 and 1.28 m slightly exceed that at 0.78 m. These observations are consistent with the evolution of a wetting front and divergence (spreading) of the flows with depth. Unsaturated zone flow is influenced by prevailing atmospheric conditions and transmissive properties of the soil matrix. After this pulse of applied moisture, soil water storage recedes very quickly (<3 d) towards its residual (baseline) state. Groundwater levels recede slowly (~1 mm d^{-1}) over this period and exhibit diurnal variations associated with variations in barometric pressure.

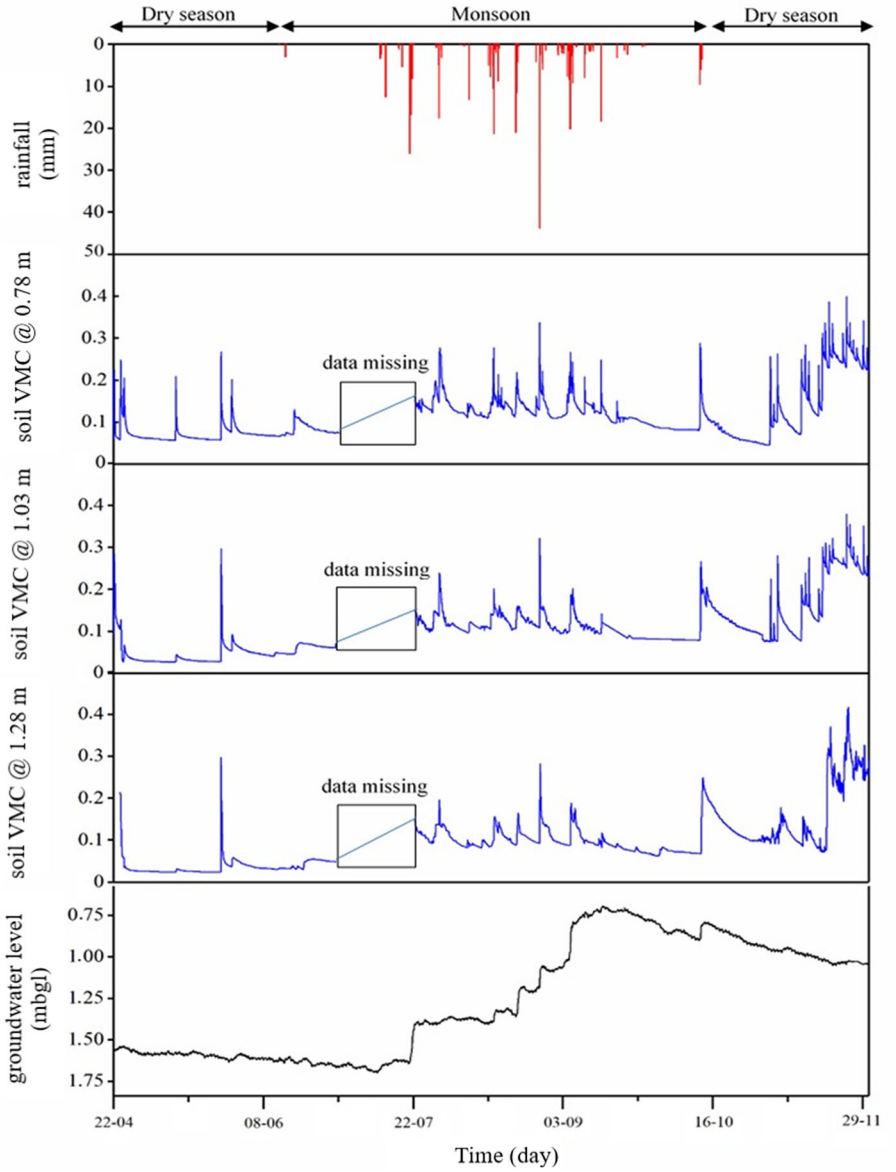

FIGURE 3 Hourly variation of the volumetric water content (VMC, in cm^3 cm^{-3}) in the unsaturated zone and groundwater level as a function of rainfall and septic tank fluxes from 22 Apr. to 30 Nov. 2020. mbgl, meters below ground level

Figure 5 presents hourly variations in rainfall, soil moisture with depth, and groundwater levels during the 2020 rainy season from 12 June to 14 October; an interruption in the monitoring of soil moisture occurred from 30 June to 22 July 2020. Total rainfall over this period was 502 mm; the number of recorded days of rainfall was 42. Rainfall intensities were predominantly (93%) under 10 mm h^{-1} (Figure 6a). As per the index of Zhou & Zhao (2021), 6 h of "heavy rainfall" (between 10 and 20 mm h^{-1}) and 4 h of "extreme rainfall" (>20 mm h^{-1}) were also observed on 21 July, as well as 14, 20, and 27 August. The duration of rainfall on individual rain days ranges from 1 to 15 h (Figure 6b); daily rainfalls occurring over periods of >10 h were recorded on 21 July (76 mm) and 5 September (46 mm). Distinct rises in soil moisture content ($N = 24$) are observed with amplitudes ranging from 0.01 to 0.22. The timing and intensity of these peaks primarily coincide with heavy and extreme rainfall events. Sharp recessions in soil moisture content, especially at shallowest monitored depth (0.78 m), reflect more rapid infiltration over shorter periods (e.g., 27 August). Longer duration rainfall events (e.g., 5 September) produce peaks with slower recessions, most notably at deeper monitored depths (1.03 and 1.28 m). Of note is that positive deflections in groundwater levels associate most strongly with periods of heavy (5 September) and extreme rainfall (21 July, 27 August).

Figure 7 presents the results of soil moisture and groundwater-level monitoring after the monsoon during the dry season from 14 Oct. 2020 to 31 Mar. 2021. In absence of rainfall and effluent from toilets until 2 Nov. 2020, when students returned to school, soil moisture content receded at

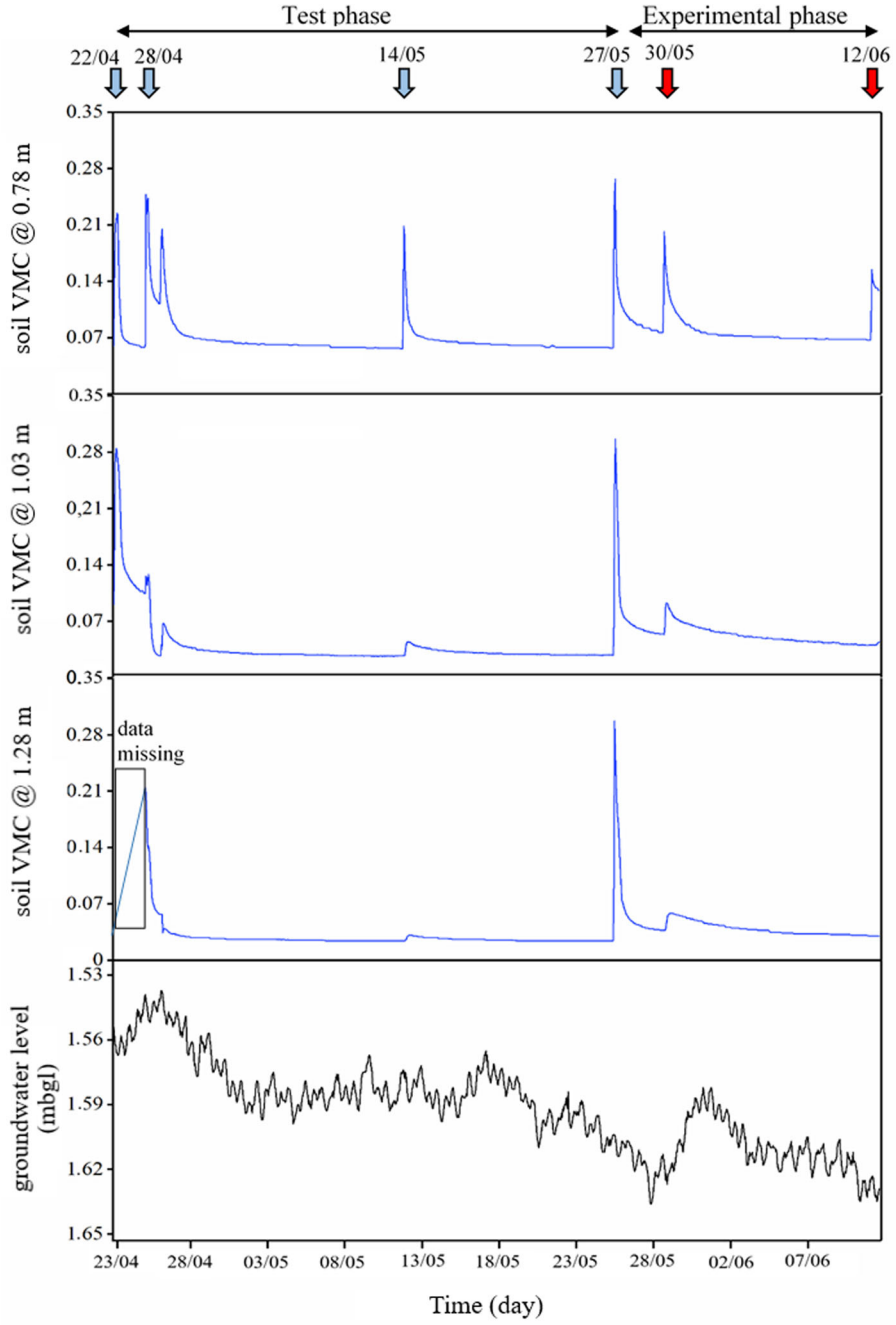

FIGURE 4 Hourly variation of the volumetric water content (VMC, in $cm^3\ cm^{-3}$) in the unsaturated zone and groundwater level as a function of septic tank fluxes during dry season (22 Apr. to 11 June 2020). mbgl, meters below ground level

all three depths. The onset of classes led to the release effluent, often before school (8:00 a.m.) and at the lunch period (12:00 p.m.), which is the busiest period during which the toilets are used. These diurnal variations in soil moisture content, absent or less pronounced during the weekend, reflect the water dynamics driven by episodic anthropogenic fluxes. Daily use of the toilets leads to sustained increases in soil moisture content (0.2–0.4) but does not induce evidence of recharge as groundwater levels recede (~2 mm d^{-1}).

3.2 | Simulated hydrological changes through the unsaturated zone during the monsoon

3.2.1 | Calibration of Hydrus-1D model

Figure 8a shows the soil water retention curves at different depths generated by field measurements where VG parameters were firstly assessed. However, the Hydrus-1D

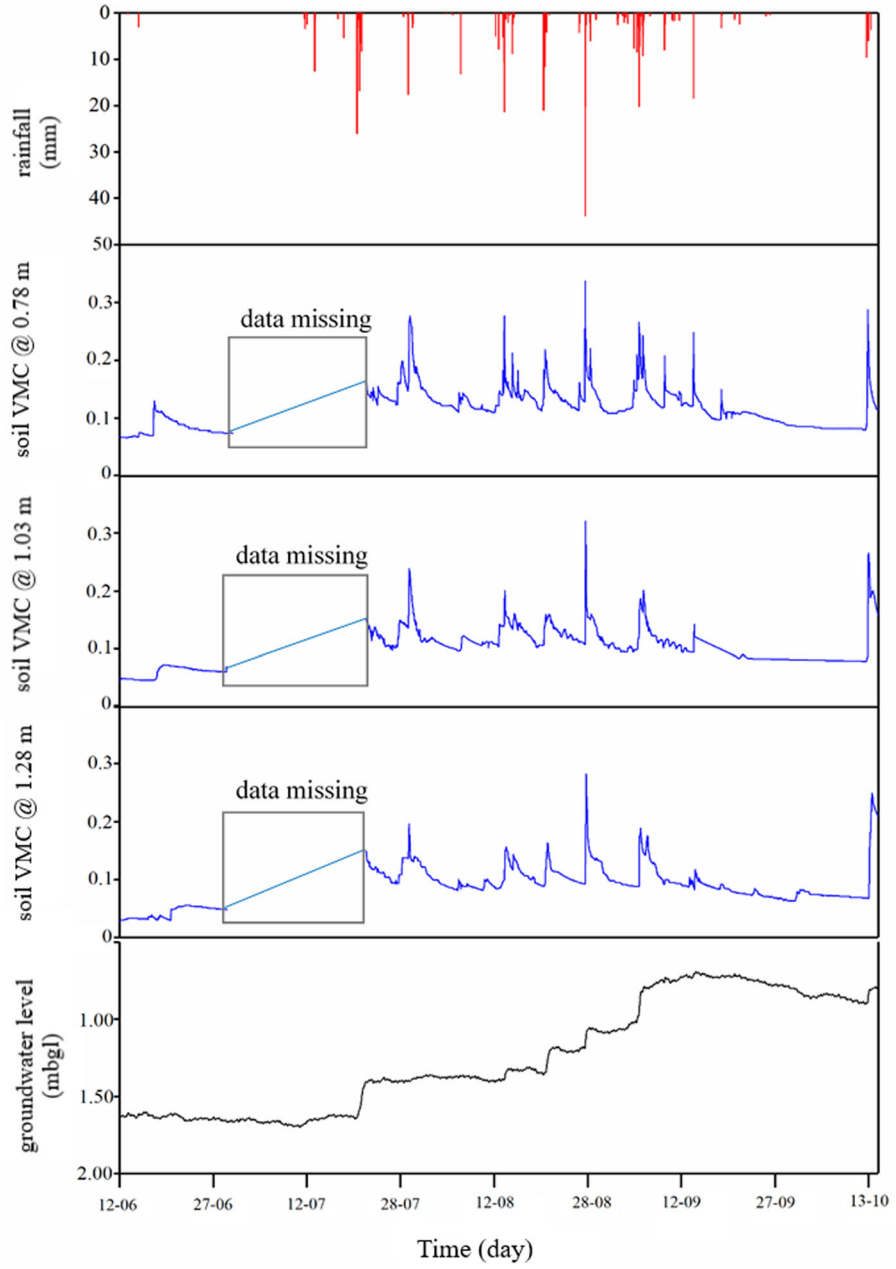

FIGURE 5 Hourly variation of the volumetric water content (VMC, in $cm^3\ cm^{-3}$) in the unsaturated zone and groundwater level as a function of rainfall and septic tank fluxes during monsoon (13 June to 14 July 2020). mbgl, meters below ground level

simulation during the 2020 monsoon provided a reasonable but unsatisfactory fit to observations (R^2 = .77–.8; RMSE = 0.015–0.033). Therefore, hourly VMC data observed during the first rainfall events of 2020 (12–22 June 2020) at 0.78, 1.03, and 1.28 m were used to optimize VG parameters applying inverse methods outlined in the Methods (Section 2.2.2). A substantially improved correlation was subsequently found between simulated and measured VMC during the calibration period (R^2 = .94; RMSE = 0.003; Figure 8b). Optimized hydraulic parameters (Table 3) were then used for model simulations.

3.2.2 | Validation of Hydrus-1D model

The VMC recorded at 0.78, 1.03, and 1.28 m from 22 July to 12 October was used to validate the calibrated model. The application of the optimized hydraulic parameters produces temporal variations in water dynamics through the unsaturated zone, with similarly strong performances with depth. In the upper horizon (0.78 m), model performance is slightly lower (RMSE = 0.019; R^2 = .79) than the subjacent horizons at 1.03 and 1.28 m (RMSE = 0.012; R^2 = .82 – .83; Figure 9).

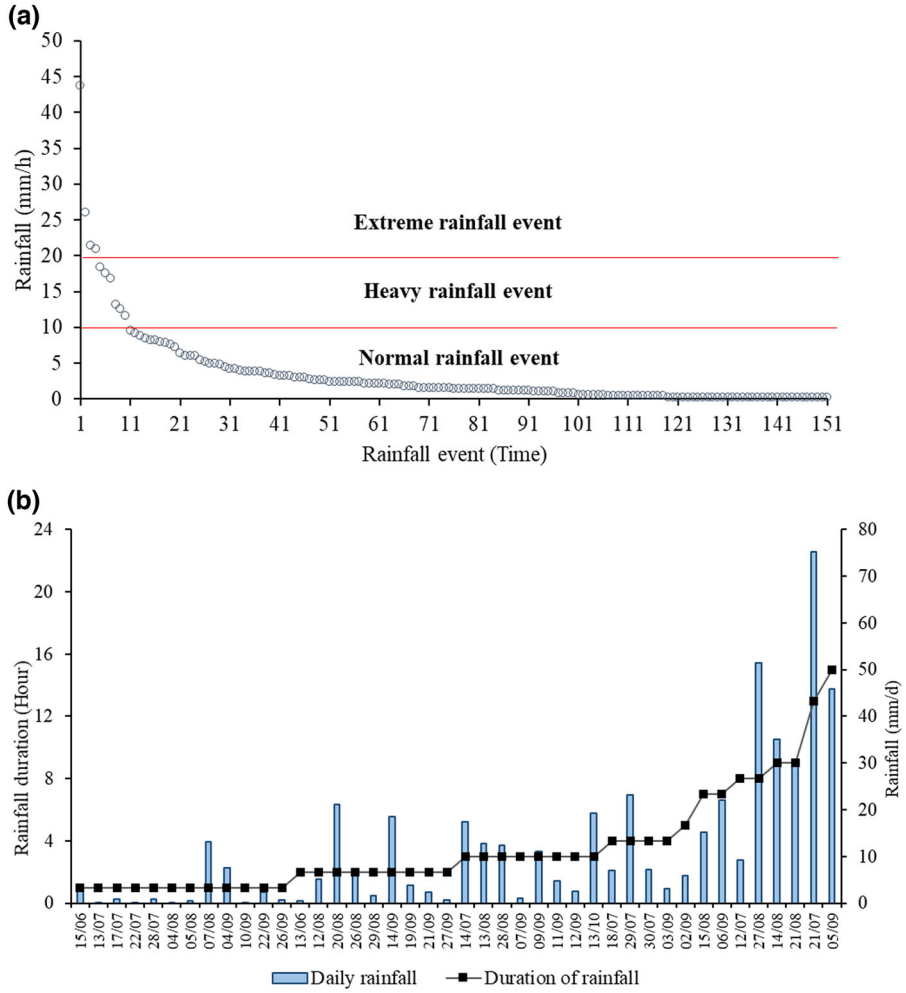

FIGURE 6 (a) Hourly rainfall distribution in 2020 according Zhou et al. classification. (b) Daily rainfall event and duration in 2020. mbgl, meters below ground level

TABLE 3 The van Genuchten–Mualem (VG) parameters based on RETC model or inverse solution

	Experimental data (RETC)			Inverse solution calibration/optimization		
VG model parameter	**0.78 m soil depth**	**1.03 m soil depth**	**1.28 m soil depth**	**0.78 m soil depth**	**1.03 m soil depth**	**1.28 m soil depth**
θ_r, $cm^3\ cm^{-3}$	0.038	0.014	0.012	0.024	0.005	0.010
θ_s, $cm^3\ cm^{-3}$	0.41	0.42	0.4	0.43	0.41	0.39
n	2.46	1.87	1.81	2.05	1.94	2
α, cm^{-1}	0.028	0.049	0.049	0.03	0.023	0.02

Hydrus-1D predicts sharp increase of VMC when heavy to extreme rainfall events occurred. During extreme rainfall events in 2020 (29 June; 14, 21, and 27 August and 5 September) for example, the predicted maximum VMC ranged from 0.19 to 0.25 $cm^3\ cm^{-3}$ throughout the profile. However, the predictions are very low compared with observations (from 0.26 to 0.33 $cm^3\ cm^{-3}$). This underestimation appear to be more important in the upper horizon. This would imply either a further redistribution of such rainfall amounts at the surface, or additional water certainly originating from the septic tank. This observation highlights the impact of extreme rainfall on the wastewater remobilization from the sanitation system to the groundwater.

Simulations underestimate variability in moisture content during rainfall in general and the recession that follow such inputs. At the same time, predictions show a best fit with

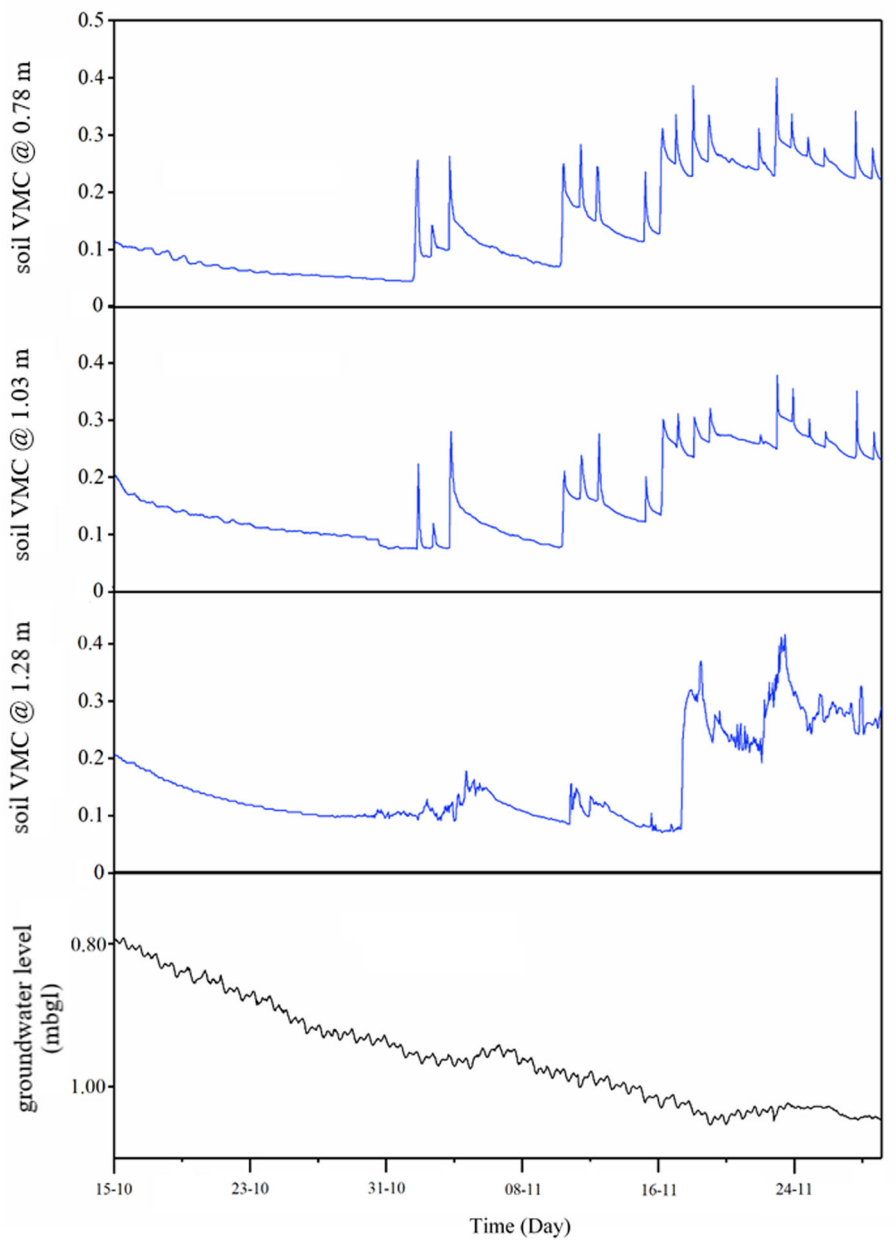

FIGURE 7 Hourly variation of the volumetric water content (VMC, in $cm^3\ cm^{-3}$) in the unsaturated zone and groundwater level as a function of rainfall and septic tank fluxes during dry season (15 July 2020 to 31 Jan. 2021)

observed values in the upper horizons when moisture content is low (0.05–0.1 $cm^3\ cm^{-3}$). This is less well observed in deeper in the profile where measurements are usually of lower levels than the predicted values. Because the surface cover at the experimental site is predominantly impermeable excluding surface cracks, neither transpiration nor evaporation were considered in unsaturated zone modeling; the potential operation of both processes may explain the difference between modelled and observed soil moisture. Heavier rainfalls are associated with more rapid increases and declines (i.e., recessions) in soil moisture.

3.3 | Nitrate variations in soil moisture during an extreme rainfall event

Time series observations of nitrate concentrations exist for a brief period preceding, during, and following the extreme intensive rainfall (43 mm h^{-1} on 27 August) in the 2020 rainy season (Figure 10). Nitrate concentrations in soil moisture, sampled at depths of 0.78, 1.03, and 1.28 m below the discharge from the toilets on 21 August, vary from 340 mg L^{-1} at 0.78 m to a high of 400 mg L^{-1} at 1.28 m. During consecutive rain days on 27 (51 mm) and 28 August (12 mm), nitrate

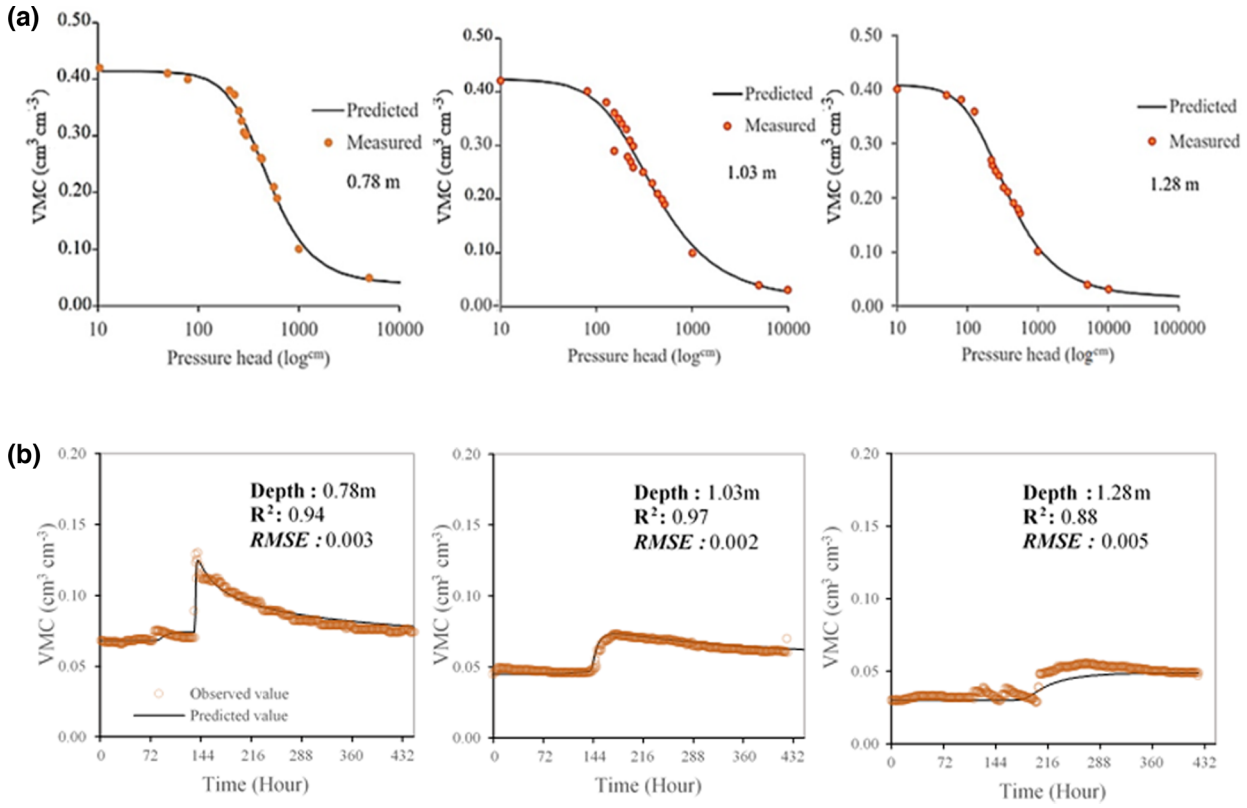

FIGURE 8 (a) Soil water retention curves modeled from observations experimental site in Keur Massar (Figure 2) at depths of 0.78, 1.03, and 1.28 m. (b) Measured vs. simulated soil volumetric water content (VMC) from 12 to 22 June 2020 (model calibration and optimization) from observations experimental site in Keur Massar (Figure 2) at depths of 0.78, 1.03, and 1.28 m

concentrations in sampled soil moisture rose more than six-fold at depths of 1.03 and 1.28 m to 2,380 and 2,630 mg L^{-1}, respectively. More modest increases, amounting to a doubling or tripling in nitrate concentrations at 0.78 m to 950 mg L^{-1} at 9:00 a.m. and 730 mg L^{-1} at 2:00 p.m. on the 28 August. On this day, nitrate concentrations in sampled soil moisture increased at 1.03 and 1.28 m from 9:00 a.m. to 2:00 p.m. Apart from a rainfall of 1.6 mm on 29 August, no other rainfall occurred until soil moisture was sampled again on 1 September. Nitrate concentrations in soil moisture on that day had receded to values less than a quarter of that observed during intensive rainfall (510 and 730 mg L^{-1} at 1.03 and 1.28 m, respectively); reductions are again more modest at 0.78 m but are consistent with the direction of trends in nitrate deeper in the profile.

4 | DISCUSSION

The present study shows that groundwater dynamics are affected specifically by heavy and extreme rainfall, which drive groundwater recharge (Boas & Mallants, 2022; Cuthbert et al., 2019; Taylor et al., 2013). Heavy and extreme rainfall (>10 mm h^{-1}) events generate recharge to the shallow groundwater table via flows consistent with matrix flow defined by the Darcy–Richards' equation. Soil physical properties investigated in this study reflect typical hydraulic parameters for sandy porous media. The VG parameters estimated here are consistent with those estimated previously by Diouf et al. (2020) in the same area, highlighting the homogeneity of the aquifer material.

Rainfall intensity and duration influence unsaturated zone hydrodynamics. Heavy and extreme rainfall events (>10 mm h^{-1}) as well as long-duration events (>5 h) lead to leaching of wastewater from the septic system and into the unsaturated zone, and instead of the expected effect of soil water dilution from infiltrating rainfall, sharp increases are observed. Variations in VMC are largely dependent on inflow and atmospheric conditions, but also on the effect of antecedent moisture as demonstrated by Cheng et al. (2018) and Boas and Mallants (2022). During extreme events, VMC increases gradually and then depends upon episodic and diversified rainfall events that clearly show a rapid evolution of the wetting front towards the water table. These dynamics are well reflected in the hydrographs with a rise in the groundwater table in proportion to extreme event intensity (Taylor et al., 2013). The near-instantaneous response of the groundwater table highlights the limits of the unsaturated zone in terms

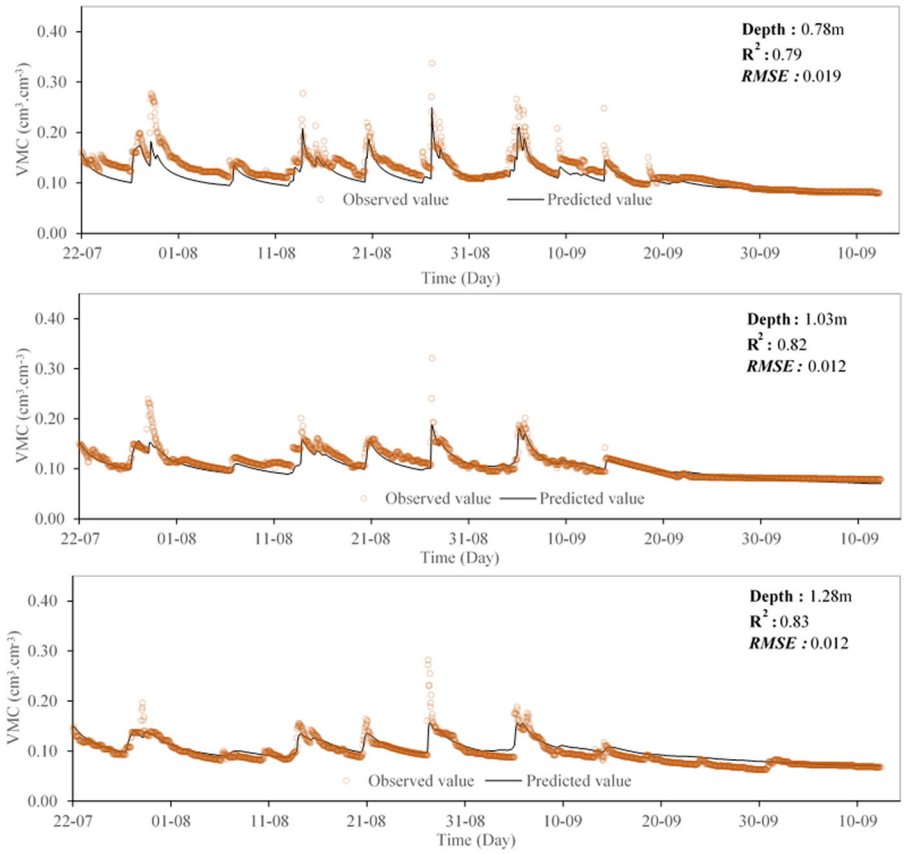

FIGURE 9 Measured vs. simulated soil volumetric water content (VMC) from 22 July to 12 Oct. 2020 (model validation) at the experimental site in Keur Massar (Figure 2) at depths of 0.78, 1.03, and 1.28 m

of storage, which is typical of shallow unconfined sandy aquifers.

During the VMC recession, observed data are lower than prediction during the recession phase. The absence of root uptake as well as evapotranspiration may play an important role in the depletion of the soil water storage. Water storage depletion in the unsaturated zone is fast; rapid recessions observed after each inflow show that the water residence time in this zone is very short (~3 d). Nevertheless, this time appears to be sufficient to initiate the mineralization of organic matter and mobilize large quantities of nitrate in these layers. The chemical processes of organic N species transformation are considered to be dominated by the hydrolysis of organic N and urea, the main components of septic tank effluents (Lusk et al., 2017).

Fecal sludge and septic tank effluent have low concentrations of nitrate. Thus, high amounts of nitrate measured in porewater suggest that nitrification of reduced forms of N is triggered by wastewater release through the sandy unsaturated zone. The magnitude of the increase in nitrate concentrations rises towards deeper soil horizons and the availability of total organic carbon. These dynamics are driven by heavy and extreme rainfalls generating rapid soil water flow towards groundwater. Similar observations have been shown by Varnier et al. (2017) who relate incomplete nitrification to a fast pulse through unsaturated zone caused by an exceptionally high recharge event. In the Thiaroye aquifer, however, attenuation of nitrate concentrations by soil water dilution as reported by Pang et al. (2006) is not observed and heavy rainfall sharply increases nitrate concentrations (three- to sixfold from ~400 mg L^{-1}) in soil moisture. These excessive nitrate concentrations are thought to result from ammonium oxidation; effluent organic matter in sandy soils may also facilitate ammonium adsorption. Whether adsorbed N plays an important role in nitrification processes and flushing of nitrate specifically observed in response to heavy rainfall is the subject of further research.

Observed variations in nitrate concentrations in the unsaturated zone of the experimental site in a low-income suburb of Dakar (Keur Massar) show that septic tanks can be a source of substantial loading of aqueous N in the form of nitrate to the subsurface. Our observations follow previous research at this location and the surrounding area that identifies the fecal source of nitrate through stable-isotope ratios of N (Diedhou et al., 2012) and in situ fluorescence spectroscopy (Sorensen, Carr, et al., 2020; Sorensen, Diaw, et al.,

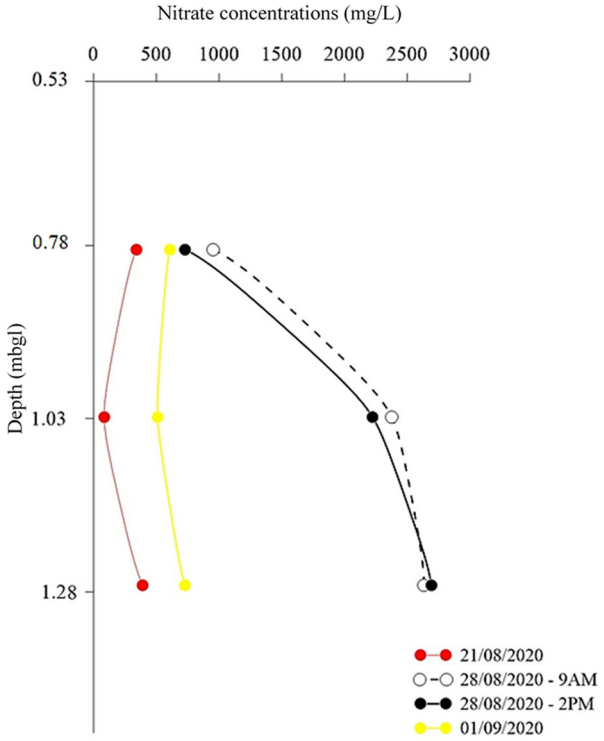

FIGURE 10 Nitrate concentrations as a function of depth in water samples collected through the unsaturated zone at the experimental site in Keur Massar (Figure 2)

2020). Critical parameters compelling nitrate contamination of shallow groundwater, beyond the form and condition of sanitation provision, are the frequency and intensity of heavy and extreme rainfall events.

5 | CONCLUSIONS

In Quaternary aeolian sands underlying a densely populated, low-income suburb of Dakar (Senegal), high-frequency monitoring of rainfall intensity, soil-moisture content and shallow groundwater levels fluctuations combined with spot sampling of nitrate and vadose zone modeling (Hydrus-1D) were conducted at an experimental site adjacent to a septic tank receiving effluent from toilets used by a primary school. Rapid increases in soil moisture content and episodic recharge contributions observed in groundwater levels caused by heavy (>10 mm h^{-1}) and extreme (>20 mm h^{-1}) rainfall are well modeled by pore-matrix flow in the unsaturated zone using the Darcy–Richards equation. Spot sampling around an extreme rainfall event in 2020 reveals a fivefold rise and fall in the concentration of nitrate in soil moisture (~500 to ~2,500 mg L^{-1}). These measurements provide new insight into the hydrological dynamics by which shallow groundwater is grossly contaminated (>500 mg L^{-1}) by nitrate through episodic flushing by heavy and extreme rainfall of wastewater from a vast network of over 250,000 septic tanks underlying suburban Dakar. Further, the outcomes emphasize the importance of effective maintenance and management of onsite sanitation, the limited capacity to attenuate wastewater from onsite sanitation systems where groundwater levels are shallow, and the vulnerability of shallow groundwater underlying onsite sanitation systems to contamination from heavy and extreme rainfall.

AUTHOR CONTRIBUTIONS

Abdoulaye Pouye: Conceptualization; Data curation; Investigation; Methodology; Software; Writing – original draft. Seynabou Cissé Faye: Supervision; Validation; Visualization; Writing – review & editing. Mathias Diedhiou: Supervision; Validation; Visualization. Cheikh Becaye Gaye: Funding acquisition; Resources; Supervision; Validation; Visualization. Richard G. Taylor: Funding acquisition; Project administration; Resources; Supervision; Validation; Visualization; Writing – review & editing.

ACKNOWLEDGMENTS

We are grateful to the ANSTS (Académie Nationale des Sciences et Techniques du Sénégal) for granting this manuscript publication charge. We are also grateful to the AfriWatSan project funded by The Royal Society Africa Capacity Building Initiative and the UK Department for International Development (DFID) (Grant Ref. AQ140023) for this document output. The views expressed and information contained in it are not necessarily those of or endorsed by the Royal Society or DFID, which can accept no responsibility for such views or information or for any reliance placed on them.

CONFLICT OF INTEREST

The authors declare that they have no competing financial interests or personal relationships that could have appeared to influence the work reported in this paper.

DATA AVAILABILITY STATEMENT

The data that support the findings of this study are available from the corresponding author, Abdoulaye Pouye, upon reasonable request.

REFERENCES

Agence Nationale de la Statistique et de la Démographie (ANSD). (2013). *Situation économique et Sociale régionale* (Final report). ANSD.

Antea-Senagrosol. (2003). *Projet Eau à long terme: etude d'impact de l'arrêt des forages de Thiaroye sur les zones basses* (Phase A Final technical report A27499/C). Antea-Senagrosol Group.

Beven, K. J., & Germann, P. F. (2013). Macropores and water flow in soils revisited. *Water Resources Research*, *49*, 3071–3092. https://doi.org/10.1002/wrcr.20156

Boas, T., & Mallants, D. (2022). Episodic extreme rainfall events drive groundwater recharge in arid zone environments of central Australia. *Journal of Hydrology*, *40*, 101005. https://doi.org/10.1016/j.ejrh.2022.101005

Cheng, Y., Zhan, H., Yang, W., & Bao, F. (2018). Deep soil water recharge response to precipitation in Mu Us sandy land of China. *Water Science and Engineering*, *11*(2), 139–146. https://doi.org/10.1016/j.wse.2018.07.007

Cissé Faye, S. (2001). *Nappe libre des sables Quaternaires Thiaroye/Beer Thialane (Dakar, Sénégal): Etude de la contamination par les nitrates sur la base d'un Système d'Information Géographique (PC ARC/INFO)*.

Cissé Faye, S., Diongue, M., Pouye, A., Gaye, C. B., Travi, Y., Wohnlich, S., Faye, S., & Taylor, R. G. (2019). Tracing natural groundwater recharge to the Thiaroye aquifer of Dakar, Senegal. *Hydrogeology Journal*, *27*, 1067–1080. https://doi.org/10.1007/s10040-018-01923-8

Cissé Faye, S., Faye, S., Wohnlich, S., & Gaye, C. B. (2004). An assessment of the risk associated with urban development in the Thiaroye area (Senegal). *Environmental Geology*, *45*, 312–322. https://doi.org/10.1007/s00254-003-0887-x

Cuthbert, M. O., Taylor, R. G., Favreau, G., Todd, M. C., Shamsudduha, M., Villholth, K. G., MacDonald, A. M., & Scanlon, B. R. (2019). Observed controls on resilience of groundwater to climate variability in sub-Saharan Africa. *Nature*, *572*, 230–234. https://doi.org/10.1038/s41586-019-1441-7

Diaw, M. T., Cissé Faye, S., Gaye, C. B., Niang, S., Pouye, A., Campos, L. C., & Taylor, R. G. (2020). On-site sanitation density and groundwater quality: Evidence from remote sensing and *in situ* observations in the Thiaroye aquifer, Senegal. *Journal of Water, Sanitation and Hygiene for Development*, *10*(4), 927–939. https://doi.org/10.2166/washdev.2020.162

Diedhiou, M., Cissé Faye, S., Diouf, O. C., Faye, S., Faye, A., Re, V., Wohnlich, S., Wisotzky, F., Schulte, U., & Maloszewski, P. (2012). Tracing groundwater nitrate sources in the Dakar suburban area : An isotopic multi-tracer approach. *Hydrological Processes*, *26*, 760770. https://doi.org/10.1002/hyp.8172

Diouf, O. C., Cissé Faye, S., Diedhiou, M., Kaba, M., Faye, S., Gaye, C. B., Faye, A., Englert, A., & Wohnlich, S. (2012). Combined uses of water-table fluctuation (WTF), chloride mass balance (CMB) and environmental isotopes methods to investigate groundwater recharge in the Thiaroye sandy aquifer (Dakar, Senegal). *African Journal of Environment Sciences and Technologies*, *6*(11), 425–437. https://doi.org/10.5897/ajest12.100

Diouf, O. C., Weihermüller, L., Diedhiou, M., Vereecken, H., Cissé Faye, S., Faye, S., & Sylla, S. N. (2020). Modelling groundwater evapotranspiration in a shallow aquifer in a semi-arid environment. *Journal of Hydrology*, *587*, 124967, https://doi.org/10.1016/j.jhydrol.2020.124967

Favreau, G., Cappelaere, B., Massuel, S., Leblanc, M., Boucher, M., Boulain, N., & Leduc, C. (2009). Land clearing, climate variability and water resources increase in Southwest Niger: A review. *Water Resources Research*, *45*, W00A16. https://doi.org/10.1029/2007WR006785

Gaye, C. B., & Tindimugaya, C. (2019). Challenges and opportunities for sustainable groundwater management in Africa. *Hydrogeology Journal*, *27*(3), 1099–1110. https://doi.org/10.1007/s10040-018-1892-1

Goni, I. B., Taylor, R. G., Favreau, G., Shamsudduha, M., Nazoumou, Y., & Ngounou, B. N. (2021). Groundwater recharge from heavy rainfall in the southwestern Lake Chad basin: Evidence from isotopic observations. *Hydrological Sciences Journal*, *66*(8), 1359–1371. https://doi.org/10.1080/02626667.2021.1937630

Kotchoni, D. O. V., Vouillamoz, J. M., Lawson, F. M. A., Adjomayi, P., Boukari, M., & Taylor, R. G. (2019). Relationships between rainfall and groundwater recharge in seasonally humid Benin: A comparative analysis of long-term hydrographs in sedimentary and crystalline aquifers. *Hydrogeology Journal*, *27*, 447–457. https://doi.org/10.1007/s10040-018-1806-2

Kulabako, N. R., Nalubega, M., & Thunvik, R. (2007). Study of the impact of land use and hydrogeological settings on the shallow groundwater quality in a peri-urban area of Kampala, Uganda. *Science of the Total Environment*, *381*(1–3), 180–199. https://doi.org/10.1016/j.scitotenv.2007.03.035

Lapworth, D. J., Nkhuwa, D. C. W., Okotto-Okotto, J., Pedley, S., Stuart, M. E., Tijani, M. N., & Wright, J. (2017). Urban groundwater quality in sub-Saharan Africa: Current status and implications for water security and public health. *Hydrogeology Journal*, *25*, 1093–1116. https://doi.org/10.1007/s10040-016-1516-6

Lusk, M. G., Toor, G. S., Yang, Y., Mechtensimer, S., De, M., & Obreza, T. A. (2017). A review of the fate and transport of nitrogen, phosphorus, pathogens, and trace organic chemicals in septic systems. *Critical Reviews in Environmental Science and Technology*, *47*(7), 455–541. https://doi.org/10.1080/10643389.2017.1327787

Madioune, D. H., Cissé Faye, S., & Faye, S. (2011). Etude de la vulnérabilité intrinsèque à la pollution de la nappe libre des sables quaternaires de thiaroye par la méthode DRASTIC. *Journal of Science and Technology*, *9*(2), 1–11.

Nayebare, J. G., Owor, M. M., Kulabako, R., Campos, L. C., Fottrell, E., & Taylor, R. G. (2020). WASH conditions in a small town in Uganda: How safe are on-site facilities? *Journal of Water, Sanitation and Hygiene for Development*, *10*(1), 96–110. https://doi.org/10.2166/washdev.2019.070

Okotto-Okotto, J., Okotto, L., Price, H., Pedley, S., & Wright, J. A. (2015). Longitudinal study of long-term change in contamination hazards and shallow well quality in two neighbourhoods of Kisumu, Kenya. *International Journal of Environmental Research and Public Health*, *12*, 4275–4291. https://doi.org/10.3390/ijerph120404275

Owor, M., Taylor, R. G., Tindimugaya, C., & Mwesigwa, D. (2009). Rainfall intensity and groundwater recharge: Evidence from the upper Nile basin. *Environmental Research Letters*, *4*, 035009. https://doi.org/10.1088/1748-9326/4/3/035009

Pang, L., Nokes, C., Šimůnek, J., Hector, R., & Kikkert, H. (2006). Modeling the impact of clustered septic tanks systems on groundwater quality. *Vadose Zone Journal*, *5*, 599–609. https://doi.org/10.2136/vzj2005.0108

Re, V., Faye, C., S, F., Faye, S., Gaye, C. B., Sacchi, E., & Zuppi, G. M. (2010). Water quality decline in coastal aquifers under anthropic pressure: The case of a suburban area of Dakar (Senegal). *Environmental Monitoring and Assessment*, *172*, 605–622. https://doi.org/10.1007/s10661010-1359-x

Schaap, M. G., Leij, F. J., & van Genuchten, M. Th. (2001). Rosetta: A computer program for estimating soil hydraulic parameters with hierarchical pedotransfer functions. *Journal of Hydrology*, *251*, 163–176. https://doi.org/10.1016/S0022-1694(01)00466-8

Seddon, N., Smith, A., Smith, P., Key, I., Chausson, A., Girardin, C., House, J., Srivastava, S., & Turner, B. (2021). Getting the message right on nature-based solutions to climate change. *Global Change Biology*, *27*(8), 1518–1546. https://doi.org/10.1111/gcb.15513

Šimůnek, J., & Hopmans, J. W. (2002). Parameter optimization and nonlinear fitting. In J. H. Dane, & G. C. Topp (Eds.), *Methods of soil*

analysis. Part 1: Physical methods (3rd ed., pp. 139–157). SSSA. https://doi.org/10.2136/sssabookser5.4.c7

Šimůnek, J., Šejna, M., Sakai, M., Saito, H., & van Genuchten, M. Th. (2008). *The HYDRUS-1D software package for simulating the one-dimensional movement of water, heat, and multiple solutes in variably-saturated media, version 4.0x, HYDRUS-1D series 3*. University of California Riverside.

Šimůnek, J., van Genuchten, M. Th., & Šejna, M. (2016). Recent developments and applications of the HYDRUS-1D computer software packages. *Vadose Zone Journal*, *15*(7), https://doi.org/10.2136/vzj2016.04.0033

Sorensen, J. P. R., Carr, A. F., Nayebare, J., Diongue, D. M. L., Pouye, A., Roffo, R., Gwengweya, G., Ward, J. S. T., Kanoti, J., Okotto-Okotto, J., van der Marel, L., Ciric, L., Faye, S. C., Gaye, C. B., Goodall, T., Kulabako, R., Lapworth, D. J., MacDonald, A. M., Monjerezi, M., … Taylor, R. G. (2020). Tryptophan-like and humic-like fluorophores are extracellular in groundwater: Implications as real-time faecal indicators. *Scientific Reports, Nature*, *10*(1), 15379. https://doi.org/10.1038/s41598-020-72258-2

Sorensen, J. P. R., Diaw, M. T., Pouye, A., Roffo, R., Diongue, D. M. L., Cissé Faye, S., Gaye, C. B., Fox, B. G., Goodall, T., Lapworth, D. J., MacDonald, A. M., Reade, D. S., Ciric, L., & Taylor, R. G. (2020). In-situ fluorescence spectroscopy indicates total bacterial abundance and dissolved organic carbon. *Science of the Total Environment*, *738*, 139419. https://doi.org/10.1016/j.scitotenv.2020.139419

Sorensen, J. P. R., Nayebare, J., Carr, A. F., Lyness, R., Campos, L. C., Ciric, L., Goodall, T., Kulabako, R., Rushworth Curran, C. M., MacDonald, A. M., Owor, M., Read, D. S., & Taylor, R. G. (2021). In-situ fluorescence spectroscopy is a more rapid and resilient indicator of faecal contamination risk in drinking water than faecal indicator organisms. *Water Research*, *206*, 117734. https://doi.org/10.1016/j.watres.2021.117734

Tandia, A. A. (2000). *Origine, évolution et migration des formes de l'Azote minéral dans les aquifères situés sous environnement péri-urbain non assaini: Cas de la nappe des sables quaternaires de Dakar (SENEGAL)* [Doctoral dissertation, Universite Cheikh Anta Diop].

Taylor, R. G., Miret-Gaspa, M., Tumwine, J., Mileham, L., Flynn, R., Howard, G., & Kulabako, R. (2009). Increased risk of diarrhoeal diseases from climate change: Evidence from communities supplied by groundwater in Uganda. In *Groundwater and climate in Africa. Proceedings of the Kampala Conference* (Vol. 334, pp. 15–19). IAHS Press.

Taylor, R. G., Todd, M., Kongola, L., Nahozya, E., Maurice, L., Sanga, H., & MacDonald, A. (2013). Evidence of the dependence of groundwater resources on extreme rainfall in East Africa. *Nature Climate Change*, *3*, 374–378. https://doi.org/10.1038/nclimate1731

Twinomucunguzi, F. R. B., Nyenje, P. M., Kulabako, R. N., Semiyaga, S., Foppen, J. W., & Kansiime, F. (2020). Reducing groundwater contamination from on-site sanitation in peri-urban sub-Saharan Africa: Reviewing transition management attributes towards implementation of water safety plans. *Sustainability*, *12*(10), 4210. https://doi.org/10.3390/su12104210

Varnier, C., Hirata, R., & Aravena, R. (2017). Examining nitrogen dynamics in the unsaturated zone under an inactive cesspit using chemical tracers and environmental isotopes. *Applied Geochemistry*, *78*, 129–138. https://doi.org/10.1016/j.apgeochem.2016.12.022

World Bank (2020). *Development report 2020*. The World Bank Group. https://ideas.repec.org/s/wbk/wbpubs.html

Xu, C., McDowell, N. G., Fisher, R. A., Wei, L., Sevanto, S., Christoffersen, B. O., Weng, E., & Middleton, R. S. (2019). Increasing impacts of extreme droughts on vegetation productivity under climate change. *Nature Climate Change*, *9*(12), 948–953. https://doi.org/10.1038/s41558-019-0630-6

Zhou, H., & Zhao, W. Z. (2021). Evolution of soil-water states in the vadose zone of a desert soil after an extreme rainfall event and its impact on the ecosystem. *Hydrogeology Journal*, *29*, 2127–2147. https://doi.org/10.1007/s10040-021-02372-6

How to cite this article: Pouye, A., Cissé Faye, S., Diédhiou, M., Gaye, C. B., & Taylor, R. G. (2023). Nitrate contamination of urban groundwater and heavy rainfall: Observations from Dakar, Senegal. *Vadose Zone Journal*, e20239. https://doi.org/10.1002/vzj2.20239